UNIVERSIDAD DE CHILE
FACULTAD DE CIENCIAS FÍSICAS Y MATEMÁTICAS
DEPARTAMENTO DE INGENIERÍA ELÉCTRICA

REDUCED BIAS CONTROL ELECTRONICS FOR SIS MIXERS IN LARGE-FORMAT HETERODYNE ARRAY RECEIVERS

TESIS PARA OPTAR AL GRADO DE
MAGISTER EN CIENCIAS DE LA INGENIERÍA MENCIÓN INGENIERÍA ELÉCTRICA

PABLO ANDRÉS TAPIA UGARTE

PROFESOR GUÍA:
PATRICIO MENA MENA

MIEMBROS DE LA COMISIÓN:
URS GRAF
MARCOS DÍAZ QUEZADA

SANTIAGO DE CHILE
MAYO 2015

Contents

Chapter 1

Introduction

The Cerro Chajnantor Atacama Telescope (CCAT) will be a 25-meter telescope for submillimeter astronomy located at 5,600 m altitude on Cerro Chajnantor in northern Chile. The upcoming construction of CCAT will bring enormous challenges to astronomical instrumentation. CCAT combines high sensitivity, a wide field of view, and a broad wavelength range to provide an unprecedented capability for deep, large-area, multicolor submillimeter surveys. Included in the instrumentation needed for this project is the CCAT Heterodyne Array Instrument (CHAI), a modular, dual-frequency band array high-spectral resolution receiver. This is intended to be the first heterodyne array receiver with 64 (baseline) and 128 pixels (goal), substantially larger than any of the heterodyne array instruments currently in operation [1] [2].

Large format heterodyne array receivers can only be built if it is possible to massively reduce the complexity of each receiver pixel. In this context the University of Cologne decided to develop a design for the SIS-mixer bias-control electronics, which will be suitable for focal plane arrays of 100 pixels or more. The immediate goal is to build a 16-pixel prototype receiver before the construction of CHAI. For each receiver pixel, the bias-control electronics supply the high-precision mixer bias voltage, the current for the magnetic field coils to suppress the Josephson effect in the SIS-mixers, and the supply voltage for the low-noise amplifiers. All these parameters can be controlled remotely from the instrument control PC. The approach of this work relies heavily on the usage of microprocessors in order to reduce the hardware complexity and replace it by software complexity. The latter is more easily modifiable and can be reproduced more reliably. An a-priori arbitrary number of microprocessors can work in parallel, which makes this approach scalable to very large pixel numbers.

Four identical boards will work autonomously in parallel under the supervision of a fifth microprocessor, which provides fast Ethernet communication. Each prototype bias-control board can operate four pixels. The array receiver must be capable to tuning itself automatically. For this process each microprocessor will run a software to gather its mixer information. Then, the fifth processor and the control PC will make an analysis of the data and take a decision over the final mixer bias voltage. A first version of the prototype bias-control board has been designed and manufactured at the University of Cologne. After lab testing, this prototype will be deployed for field testing in the existing Sub-Milimeter Array Receiver for Two frequencies (SMART) receiver at the NANTEN2 telescope on Pampa la Bola, Chile. As part of a collaboration between the Universities of Chile and Cologne, the aim of this thesis work is to program the microprocessor of the board to interact with the mixer and thus have a basic functioning module.

1.1 Objectives

1.1.1 General Objective

Program the microprocessor of the prototype bias-control board to interact with the mixer.

1.1.2 Specific Objectives

- Design and program the software of the microprocessor.
- Test the board in a laboratory set-up.

1.2 Thesis Structure

This thesis is structured as follows.

- **Chapter 2 - Background**: Summary of the necessary concepts to understand this thesis work.
- **Chapters 3 and 4 - Methods**: Description, developing and results of the programming and testing.
- **Chapter 5 - Conclusion**: Conclusion about the proposed objectives and summary of the obtained results.

Chapter 2

Background Concepts

2.1 SIS Mixers

2.1.1 Description

The Superconductor-Insulator-Superconductor (SIS) junction, also known as superconducting tunnel junction, is an electronic device consisting of two superconductors separated by a very thin layer of insulating material. The quantum mechanical nature of SIS tunnel junctions lies in charge carriers flowing through the junction via the quantum-tunneling process. Heterodyne mixers based on quasi (single)-particle tunneling are known as SIS mixers.

The theory of quantum limited detection in superconducting tunnel junctions was presented by Tucker in 1979 [3]. The important aspects of this theory are the prediction of quantum limited mixer noise and the possibility of RF-IF conversion gain, i.e. down conversion. The sharp non-linear IV curve of the tunnel junction is key for this latter phenomenon to occur and is also responsible of frequency mixing. When two signals with different frequencies are applied to the junction, the Intermediate Frequency (IF) is produced as one of the resulting combinations. This non-linearity is explained by the semiconductor model of the excitation spectrum in a superconductor [4].

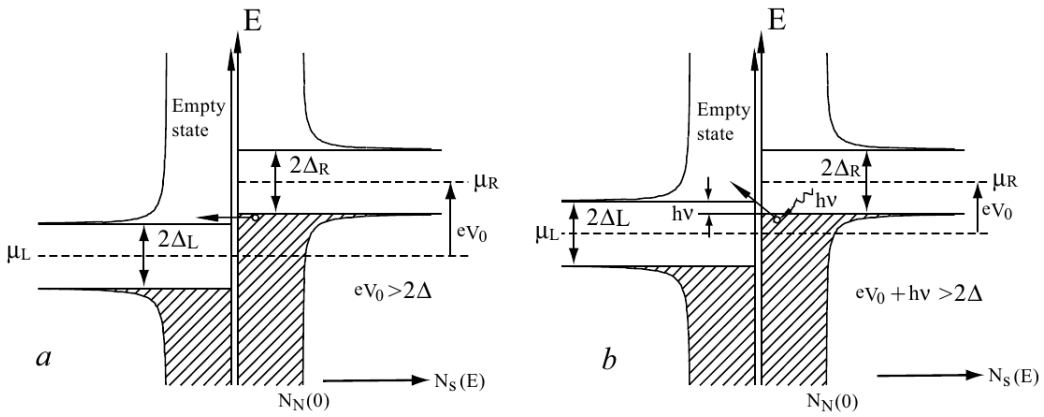

Figure 2.1: Semiconductor picture of an SIS tunnel junction. **a)**: Density of states vs. energy for quasi-particle tunneling at the same energy level. **b)**: Photon assisted tunneling. Reference: [6] "Chapter 4: Fundamentals of SIS and HEB mixers".

2.1.2 Photon-assisted Quasi-particle Tunneling

The microscopy theory of superconductivity, called the BSC theory, was formulated by Bardeen, Cooper and Schreiffer in 1957 [5]. In certain metals, due to phonon-mediated attraction, two electrons with opposite momentum and spin can form the so-called Cooper pairs. Low temperatures (T~0 K) are favorable energy-wise for these pairs to condense into the lowest energy state, called ground state. In this state, a macroscopic number of pairs interact and move in a correlated way causing the superconductivity. According to the BCS theory, the minimum excitation energy of a quasi-particle (unpaired electron) excited from the ground state is Δ. Therefore, a minimum energy of 2Δ is required to break a cooper-pair and create two quasi-particles (quasi-electron and quasi-hole) with the same momentum but in opposite directions. This breaking energy is known as the superconducting energy gap.

The onset of quasi-particle tunneling (see Fig.2.1a) takes place at DC voltage levels of $eV_0 = 2\Delta$. At those levels there is enough energy to allow a single electron to tunnel through the barrier and enter to an available quasi-particle state above the gap, leaving an unpaired quasi-hole particle behind. In the photon-assisted tunneling (see Fig. 2.1b), however, the photon energy plus the DC voltage should be higher than 2Δ for electrons to be able to tunnel.

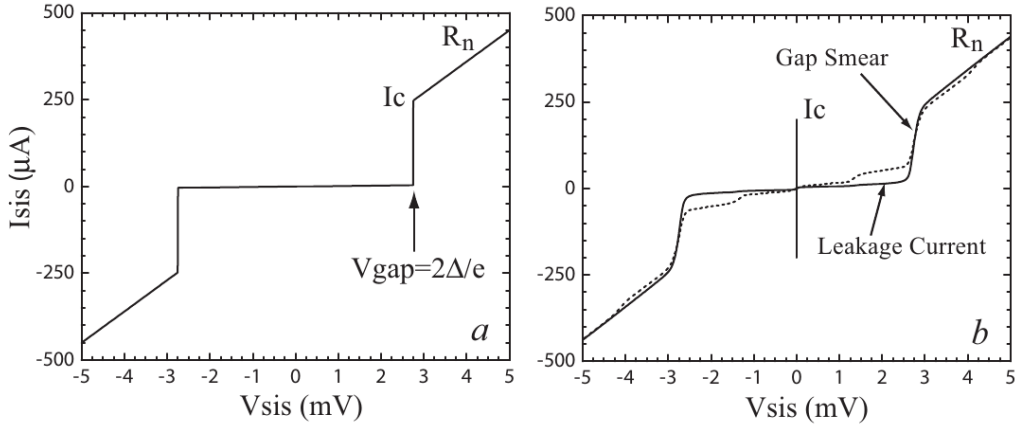

Figure 2.2: Semiconductor picture for an SIS tunnel junction. **a)**: Ideal high-current density AlN-barrier SIS I/V curve at 0 K **b)**: Real measured I/V curve. Reference: [6] "Chapter 4: Fundamentals of SIS and HEB mixers".

Fig. 2.2a shows an ideal IV curve at 0 K. The sharp rise in current at the gap voltage correspond to the divergent density of states just above and below the gap. A real SIS junction at non-zero temperature will conduct some small leakage current when biased below the gap. Fig 2.2b shows a measured IV curve of a high current density SIS junction. The parameters that define the junction are gap voltage, sub-gap leakage current, gap smearing, and the critical current (I_c). This critical current is a constant determined by the superconducting energy gap and normal state resistance of the junction, and represents the maximum possible zero-voltage tunnel current that can be driven [6] [4].

2.1.3 Josephson Effect

The potential barrier between two superconductors also supports Cooper-pair tunneling. This phenomena was discovered by B. D. Josephson in 1962 [7]. The current induced by the cooper-pair (see Equation 2.1) depends on the phase difference ϕ of the superconducting waves functions across the barriers, and the critical current I_c (see Fig. 2.2).

$$I = I_c \sin(\phi). \tag{2.1}$$

If a constant voltage is applied to the junction, the phase difference varies in time following

$$\frac{d\phi}{dt} = \frac{2eV_0}{h}. \tag{2.2}$$

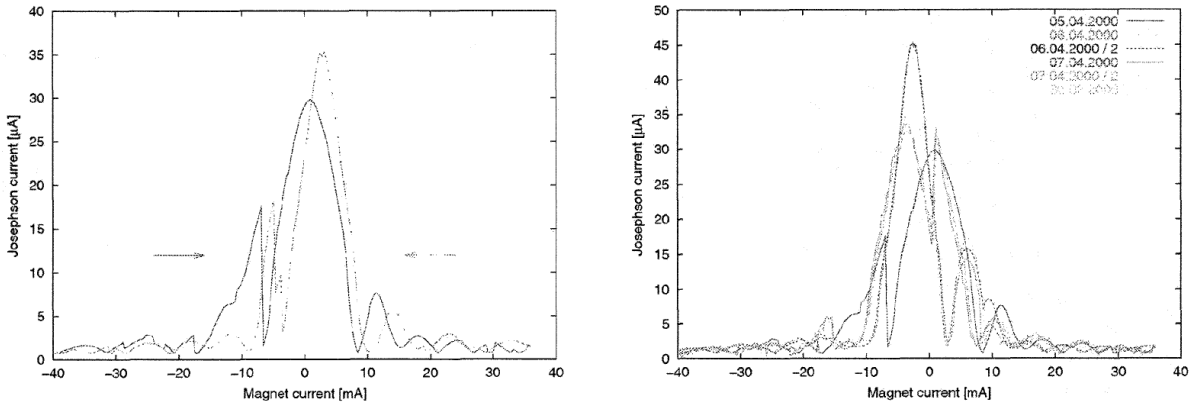

Figure 2.3: Hysteresis and statistical effects of the magnetic field scans. **Left)**: Two magnetic field scans in different directions. **Right**: Magnetic field scans on different days. Reference: [9].

This implies an oscillating current at a frequency $\nu = 2eV_0/h$, known as the "AC-Josephson effect". In an LO pumped mixer, this Josephson oscillations are excited at discrete voltages $S_n = nh\nu_{lo}/2e$ (with n an integer number), known as Shapiro steps [8]. Biasing on a Shapiro step results in a considerable amount of noise in the mixer with the subsequent unstable behavior of the receiver. However, the Cooper-pair tunneling can be supressed using a magnetic field. This is because the critical current is a function of the magnetic field flux Φ that is applied to the junction. For rectangular junctions the critical current can be describe as follows

$$I_c = I_c(0) \left| \frac{\sin(x)}{x} \right|, \; x = \frac{\pi\Phi}{\Phi_0}. \tag{2.3}$$

Fig. 2.3 shows the behavior of Josephson current (in terms of magnetic field flux) in the SIS-mixer of the SMART receiver. This experiment points out, nontheless, that the magnetic field required to suppress the Josephson current is not always reproducible due to external and statistical effects.

2.2 Bias-control System in SIS-array Receivers

In the last decade, SIS array receivers have been installed on mm- and sub-mm telescopes by different universities and research centers. Starting with PoleStar [10] and SMART [11] in 2000, DesertStar [12] and HERA [13] in 2004, to the SuperCam [14] in 2010. However, the bias-control system has been developed under the same concepts of the early projects, the advances in other areas notwithstanding.

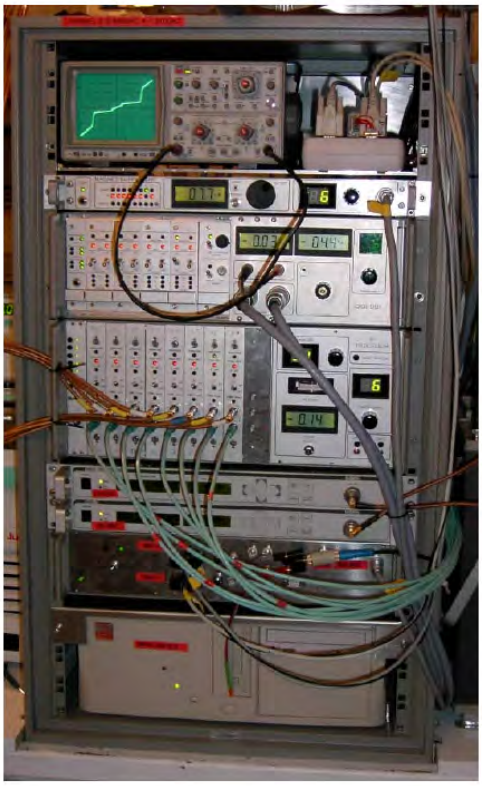

Figure 2.4: Photograph of the SMART electronics rack (left hand panel). The rack contains (from top to bottom): an oscilloscope, the magnet supply box, the mixer bias box, the IF processor box, two microwave synthesizers for the LO phase lock, the computer interface box, and the instrument control PC. Reference: [11].

Fig. 2.4 shows the bias electronics subsystems of KOSMA's array receiver (currently installed in NANTEN2). A control PC is connected to all of the other subsystems through a PC interface. This provides full control of the mixer's operating parameters through a terminal or Ethernet connection. The central units are the mixer magnet supply, the mixer bias box, and the IF processor. All of these units contain individual cards (one for each receiver channel) plus a control unit to select a channel, and to display and modify this channel's operating parameters. This bias-control electronic was designed for both manual and computer controlled operation. All the signals needed for the bias-control process have to pass the PC interface, where a switch controls whether or not the PC is connected to the subsystems. This approach made the process heavily dependent on specialized hardware [9] [11].

Even though this early approach was focused on scalability, the advances in digital electronics technology nowadays allow considerable differences in terms of implementation. Leaving aside the manual controlled operation and using microprocessor technology, it is possible to change hardware complexity into software complexity. This creates more integrated systems that are easy to modify and can be reproduced more reliably for a large amount of pixels.

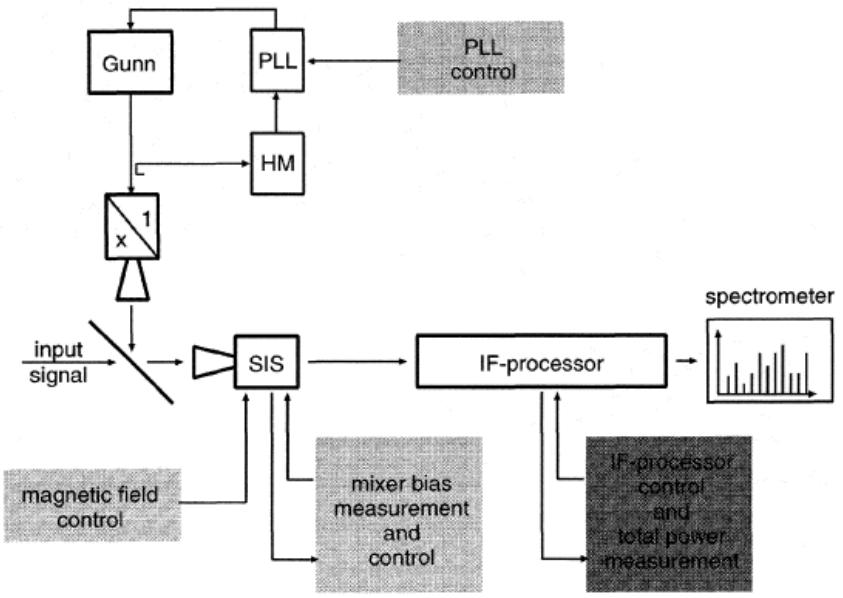

Figure 2.5: Diagram of the receiver electronics consisting of: the magnetic field control; the mixer bias measurement and control system; and the IF-processor, in which the IF total-power measurement is integrated. The shaded boxes are computer controlled. Reference: [9].

This thesis work shows how the mixer magnet supply and mixer bias box can be replaced with microprocessor functionalities, obtaining the same results when measuring the IV curve.

2.3 Tuning of SMART

This section summarizes the important concepts of the tuning of the SMART array receiver, but focused only in one pixel. The discussion reviews the article of S. Stanko, U. Graf, and S. Heyminck 2002, Automatic Tuning of SMART, KOSMA's 490/810 GHz Array Receiver [9].

Although SMART is an array receiver, each of the channels has to be tuned individually. Fig. 2.5 shows the main elements of the electronics. All of these units contain individual cards (one for each receiver channel) plus a control unit to select a channel, and to display and modify this channel's operating parameters. This bias-control electronic was designed for both manual and computer controlled operation.

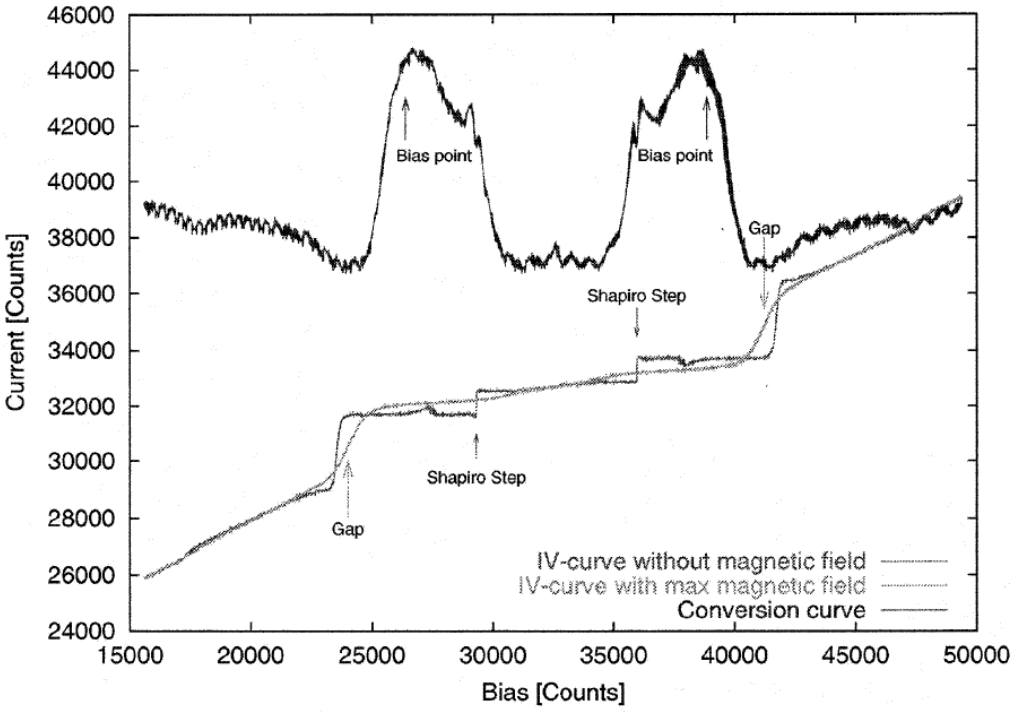

Figure 2.6: Gap voltage and bias point derived from IV-curve with high magnetic field and without. The conversion curve is shown to demonstrate the bias point. Reference: [9].

The mixer bias-control unit is the primary power supply for the junctions and their IV characteristics can be measured with this device. The magnetic field control generates the current to establish a magnetic field which is applied to the junction in order to suppress the Josephson current with its associated noise [1].

To compute the proper bias point, first the IV-curve with maximum magnetic field is recorded. The gap voltage is derived to provide a preliminary scaling of the IV-curve. Now the Shapiro step on the IV-curve (see Fig. 2.6) without any applied magnetic field is determined. This yields a very accurate calibration of the voltage scale, which is required to set accurate bias points.

[1] Due to the variability of the Josephson current presented in Fig. 2.3, it is impractical to use algorithms based on lookup tables. The correct magnetic field strength must be calculated by measuring the IV curve or the conversion curve. One method presented by S. Stanko, U. Graf and S. Heyminck in 2002 [9], consists of an algorithm that evaluates magnetic fields scans over the IV curve and conversion curve, near to the Shapiro step.

Chapter 3

Microprocessor Programming

This chapter will describe the important aspects of this work related to the microprocessor programming. First we describe how the system was set-up. This includes a first iteration of the work and the resulting design improvements. Then we describe the software architecture refers to the high-level set of structures and their relationships. Finally, we describe two functions to show how the software system works.

3.1 Setting Up the System

3.1.1 Initial Set-up

As shown in Fig. 3.1.1 the system is composed of three main sections: control (A), electronics (B) and peripheral components (C). In the Control PC (1) the instructions are read and interpreted to be sent via SPI to the microprocessor (2) in the electronic board. After the instructions arrive to the microprocessor, it will: control the access to the mixer (3) by enabling/disabling the relays (4); then configure the DAC (4) to set the objective voltages on the mixer, magnetic coil (6) and LNAs; finally configure the ADC (7) to read the voltages on the mixer and send back the readout information to the Control PC.

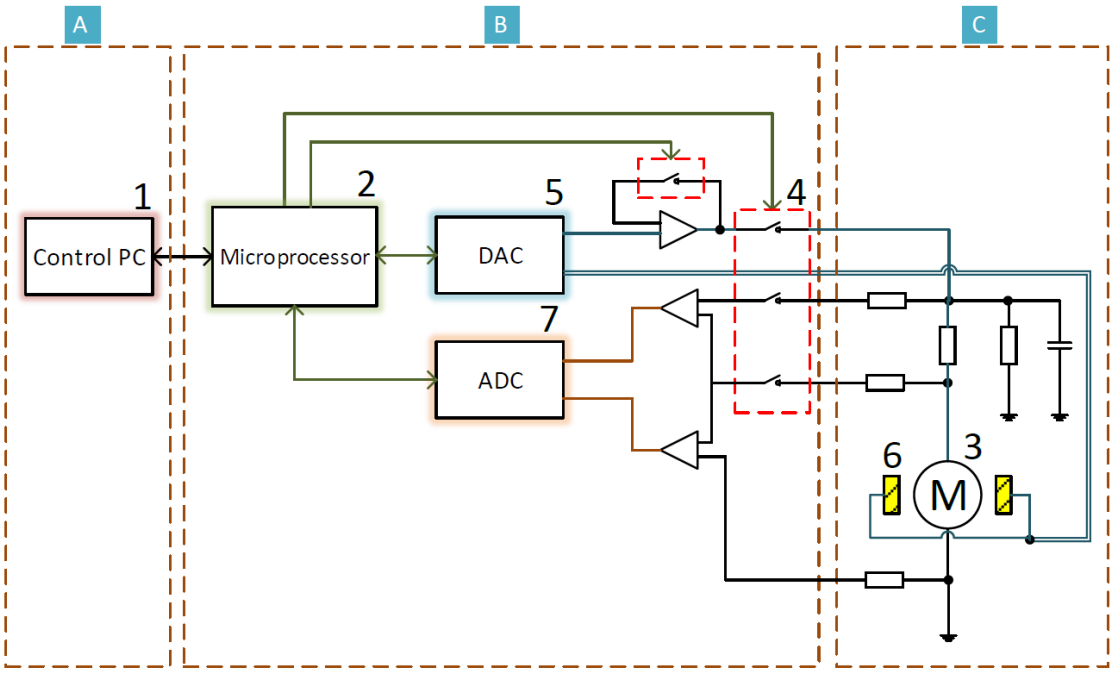

Figure 3.1.1: General diagram of the control (A), electronics (B) and peripheral components (C) system set-up.

3.1.2 Design Improvement

An initial iteration of microprocessor programming and lab testing was needed for a stable version of the hardware to work with. In this process a dangerous voltage spike on the mixer terminal was detected when activating the connection relay. The amplitude of this spike was diminished by placing a solid state relay (8) (see Fig. 3.1.1), that takes the gain of the OpAmp to the minimum possible level before the connection occurs. This situation also motivated the creation of a specific series of instructions in order to safely enable the mixer (see Section 3.3.2).

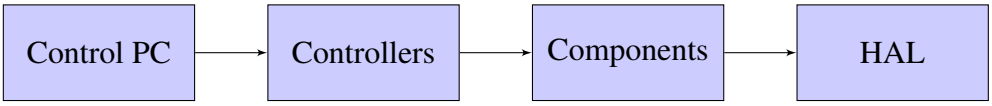

Figure 3.2.1: Architecture Diagram

3.2 Software Architecture

As shown in Fig. 3.2.1 the software is composed of four layers: Control PC, Controllers, Components and the Hardware Access Layer (HAL).

- The Control PC is the layer that provides the interface for the communication of the user with the Controllers functions.
- The Controllers are high level functions that allow the user to manipulate the system in order to achieve certain objectives (e.g. make a sweep of the mixer bias voltage).
- The Components layer contains the modules to interact with the devices (mixer, LNAs & magnetic coil) through the HAL layer.
- The HAL is the lowest level layer in charge of the configuration and communication with the hardware.

3.3 Description of Important Functions

To illustrate the process two important instructions will be explained referring to the software architecture (see Fig. 3.2.1)[1].

3.3.1 Set Mixer Bias Voltage Function

This function is defined as `SET_BIAS_VOLTAGE` and aims to set up the bias voltage of the mixer in a specific value. As shown in Fig. 3.3.1, the process starts with a command typed in the Control PC with the code of the instruction and the desired value (seen in Fig. 3.3.1 as '2047'). After some technical steps, this value arrives to the mixer component module, and here it is stored in the variable `mixer_bias_value`. This module then call a function of the HAL to modify the bias voltage channel `BIAS_CH` to the recently stored value `mixer_bias_value`. After this last process ends a confirmation messages is sent back to the Control PC.

[1]For the rest of the functions please refer to hexadecimal command list in Appendix A.1

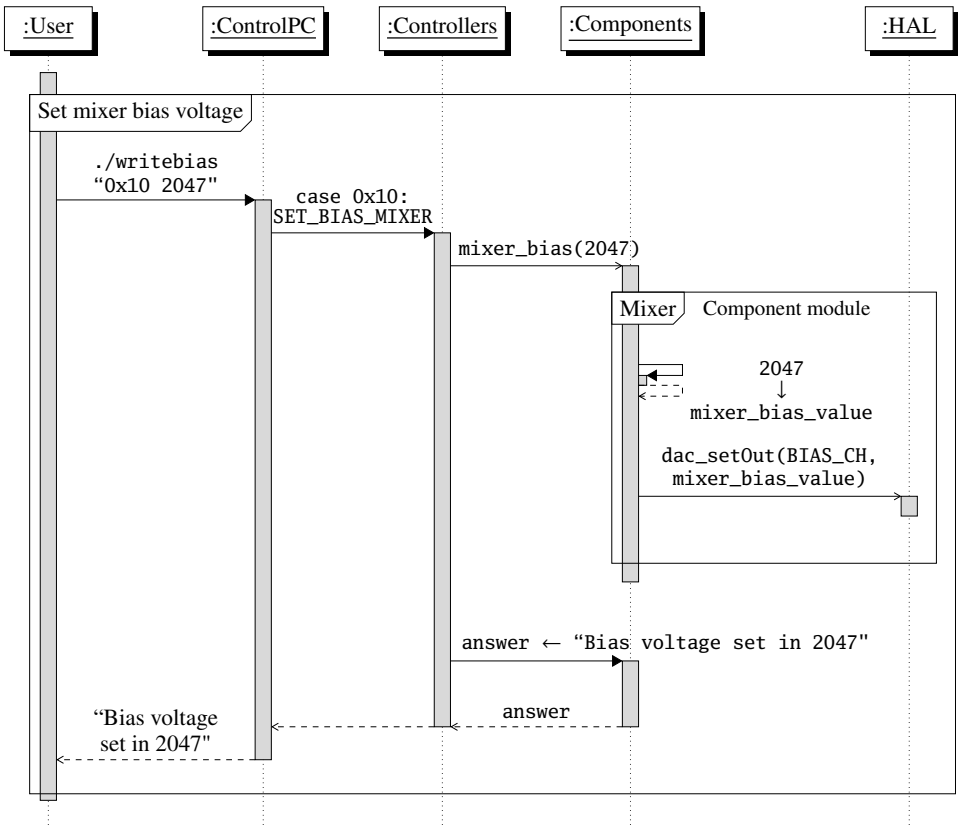

Figure 3.3.1: Instructions sequence example of setting the mixer bias voltage.

3.3.2 Enable Mixer Function

Even though the bias voltage channel is modified with the instruction explained above, there is no real effect on the mixer. The latter needs a controlled series of steps to be safely connected with the electronic, so the change can take effect. This function is definded as `ENABLE_MIXER` and aims to minimize all the voltages before the connection in order to avoid or diminish any spike in the junction with the mixer. The instructions process can be seen in Fig. 3.3.2 and what occurs inside the mixer module can be described as follows.

1. Set the DAC channel of the mixer bias voltage (`BIAS_CH`) to the minimum voltage value (`BIAS_ZERO`). As the DAC is configured to function in the ±2.5 V and has a resolution of 12 bits, the zero value is located at `2047` approximately.
2. Enable the relay `OPAMP` of the regulation OpAmp to take the gain of it to low.
3. Wait 20 ms for the relay to act.
4. Enable the relay `MIXER` that actually makes the connection between the mixer and the electronics.
5. Wait 20 ms for the relay to act.

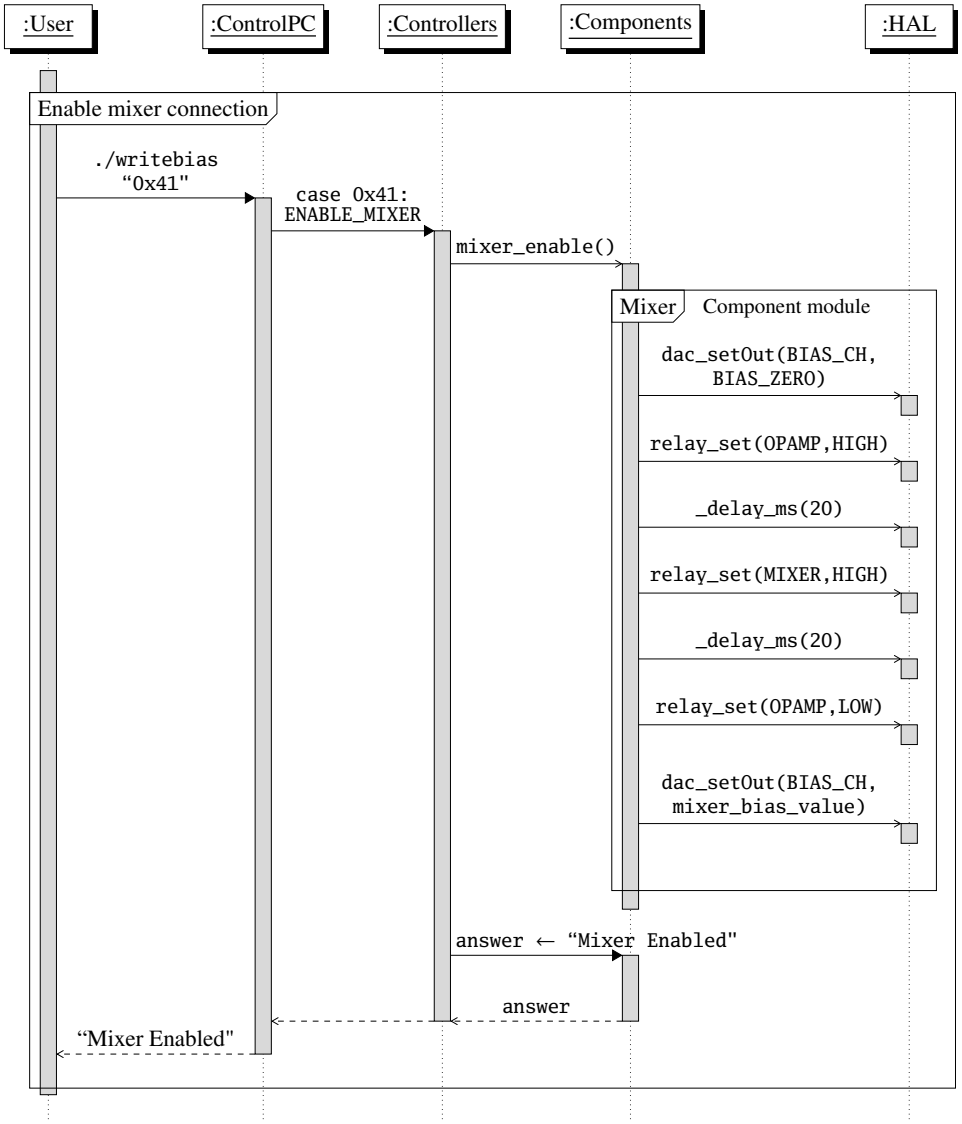

Figure 3.3.2: Instructions sequence example of enabling the mixer connection.

6. Disable the relay `OPAMP` of the regulation OpAmp to take back the gain of it to high.

7. Set the DAC channel of the mixer bias voltage to the value that is stored in the `mixer_bias_value` variable.

3.3.3 Sweep Functions

These functions are used to see the actual behavior of the mixer and to gather information to the Control PC in order to make performance analysis.

The actual sweep functions (bias and magnet sweep) are used with debugging purposes and as an early version of the scan functions. In this stage of the project it is not possible to decide the final mixer bias voltage automatically. Therefore, it is useful to have a real time response when changing the magnet field or when connecting the local oscillator. The scan functions, on the other hand, are now useful to gather information of the behavior for post-analysis of the performance. In the future, the goal is that these functions will gather information for the Control PC to analyze and then make the decision of the final bias voltage for the mixer.

- `START_BIAS_SWEEP`: Makes a continuous sweep of the mixer bias voltage between the minimum to the maximum value.
- `START_MAGNET_SWEEP`: Makes a continuous sweep of the magnet current bias voltage between the minimum to the maximum value.
- `STOP_SWEEP`: Stops the the bias/magnet sweep.
- `BIAS_SCAN`: Performs a single sweep of the mixer bias value from the minimum to the maximum value and back. After every change of mixer bias voltage value the actual mixer voltage and current are measured and sent to the Control PC.
- `MAGNET_SCAN`: Performs a single sweep of the magnet current from the minimum to the maximum value and back. After every change of magnet current value the actual mixer voltage and current are measured and sent to the Control PC.
- `BIAS_SCAN_SLOW`: Performs a single slow sweep of the mixer bias value from the minimum to the maximum value and back. After every change, a delay is included and then the actual mixer voltage and current are measured and sent to the Control PC.

Chapter 4

Laboratory Testing

This chapter will describe the software verification process by testing the board in two different environments: dummy and mixer set-up. The difference between both lies in whether the real mixer is or is not connected to the electronic board. The first environment is about checking the basic functioning of the software in a safe environment and the latter aims to obtain the IV curve of the real mixer, using just the programmed software. Finally, a performance analysis will be made measuring the time constant and evaluating his influence on the quality of the obtained data.

In thi chapter we describe the software verification process by testing the board in two different environments, a dummy and a mixer set-up. The difference between both lies in whether the real mixer is or not connected to the electronic board. The first set-up checks the basic functioning of the software in a safe environment and the latter aims to obtain the IV curve of the real mixer, using just the programmed software. Finally, we made a performance analysis by measuring the time constant and evaluating its influence on the quality of the obtained data.

4.1 Dummy Set-up

In this set-up the peripheral components (see block C in Fig. 3.1.1) were replaced by a dummy board. The aim is to protect the mixer and take advantage of the simplicity of the set-up. The verification process consisted of the following stages.

1 Check the Communication The `STATUS` function was executed in order to see the firmware information of the microprocessor. With this function it was possible to check that the board was receiving instructions from the control PC.

Table 4.1: Analog and digital values of the mixer voltage and current, corresponding to different values of the DAC determined by the Control PC.

DAC		Mixer I	ADC		Mixer V	ADC	
Value	Output V	I mA	Input V	Value	V mV	Input V	Value
0	-2.503	+0.89	-2.011	-13203	-8.7	-2.492	-16366
2054[1]	+0.0	+0.0	-0.012	-98	+0.0	+0.0	-140
4095	+2.487	-0.89	+1.975	+12925	+8.6	+2.476	+16223

2 Check the Response The `SET_BIAS_VOLTAGE` function made possible to set critical values and then use analog tools to measure the response. The `MIXER_STATUS` function was used to obtain the values measured digitally. This process can be summarized in Table 4.1 and the results were also used to check the following initial system considerations.

- The voltage on the mixer can not be higher than ±10 mV.
- The DAC has a resolution of 12 bits in a ±2.5 V voltage range.
- The ADC has a resolution of 16 bits and is configured to work in a ±5 V voltage range.

3 Enabling and Disabling the Mixer It was verified that there was no actual change in the mixer bias voltage unless the mixer was enabled, or analogously, after the disable function is used. However, it is important to note that the software variable, `mixer_bias_value`, could be modified regardless of the state of the mixer.

A tracing of the voltage of the mixer bias voltage was made using an oscilloscope. The objective was to recognize that there are no over-voltages in the complete process of enabling and disabling the mixer.

The results of both tests were satisfying. However, an actual spike was identified in the first iteration of this thesis work. This resulted in a redesign, explained in Section 3.1.2.

4 Check Sweep and Scan In this stage, the functions were tested to ensure they worked properly. The test consisted of the following steps.

1. Execute the `START_BIAS_SWEEP` instruction.

[1]The value 2054 represented values closer to zero than 2047. The complete version of this measurement can be reviewed in Appendix B.1

2. Use the oscilloscope to measure the analog values of the mixer voltage and current. Take a screenshot of the oscilloscope and store the data.

3. Execute the `STOP_SWEEP` instruction.

4. Start the scan with the `BIAS_SCAN` instruction.

5. Process the information received in the control PC and with the oscilloscope and compare them in a plot.

Although there is no record of the test in this set-up, an example of this comparison can be seen later in Fig. 4.2.3.

4.2 Mixer Set Up

In this set-up the peripheral components (see block C in Fig. 3.1.1) corresponded to the real mixer. In order to achieve the superconductor state of the mixer, it was necessary to cool down the cryostat to 4 K. The aim of this stage was to test the software in a real environment, by obtaining the IV curves of the real mixer under different conditions. The verification process consisted of the following stages.

1 Check the Communication The `STATUS` function was executed in order to see the firmware information of the microprocessor. This was done to check that the board is receiving instructions from the Control PC.

2 Check the Response The `SET_BIAS_VOLTAGE` function made possible to set critical values and then use analog tools to measure the response. The `MIXER_STATUS` function was used to obtain the values measured digitally.

3 Obtain the IV Curve For this process the sweep instruction was needed to see the real time effects on the mixer. However, after each change of the conditions, the sweep was stopped momentarily to perform a scan to record the current situation. Those measurements are shown in the Appendix B.2 as example curves of each step, excluding the final IV curve.

3.1 Initial IV Curve for the Mixer This corresponds to the IV curve of the mixer without the effects of the local oscillator or the magnetic field (see Fig. B.2.1 of Appendix B.2).

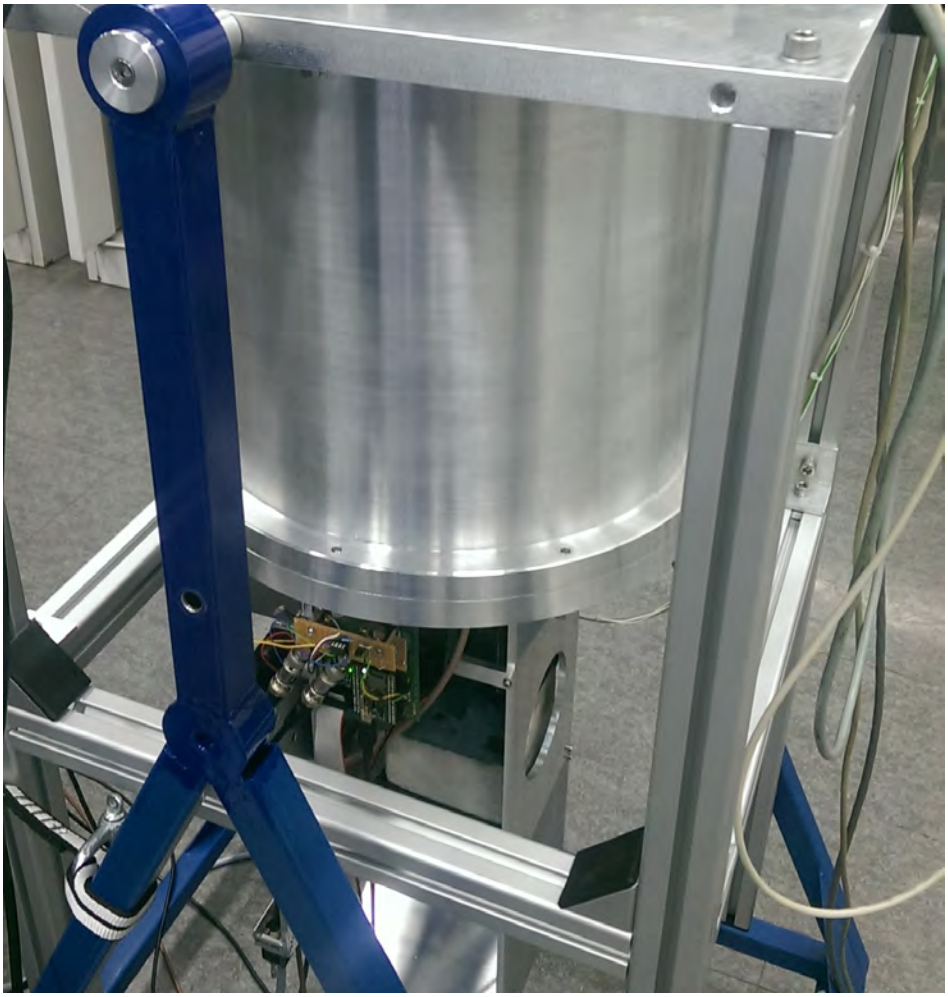

Figure 4.2.1: Mixer set-up for laboratory testing.

3.2 IV Curve with Magnetic Field Effect As explained in Section 2.1.3, the magnetic field is used to diminish the Josephson effects. While a sweep of the voltage is running in the mixer, it is possible to execute the `SET_MAGNET_CURRENT` function to change the value of the magnetic field coils current. The change of the shape of the curve could be seen in real time. A smooth version of the initial IV curve can be seen as a result of this process (see Fig. B.2.2 of Appendix B.2).

3.3 Effect of the Local Oscillator on the IV Curve This corresponds to the IV curve under the same conditions of the initial curve but with the mixer lit by the local oscillator (see Fig. B.2.3 of Appendix B.2).

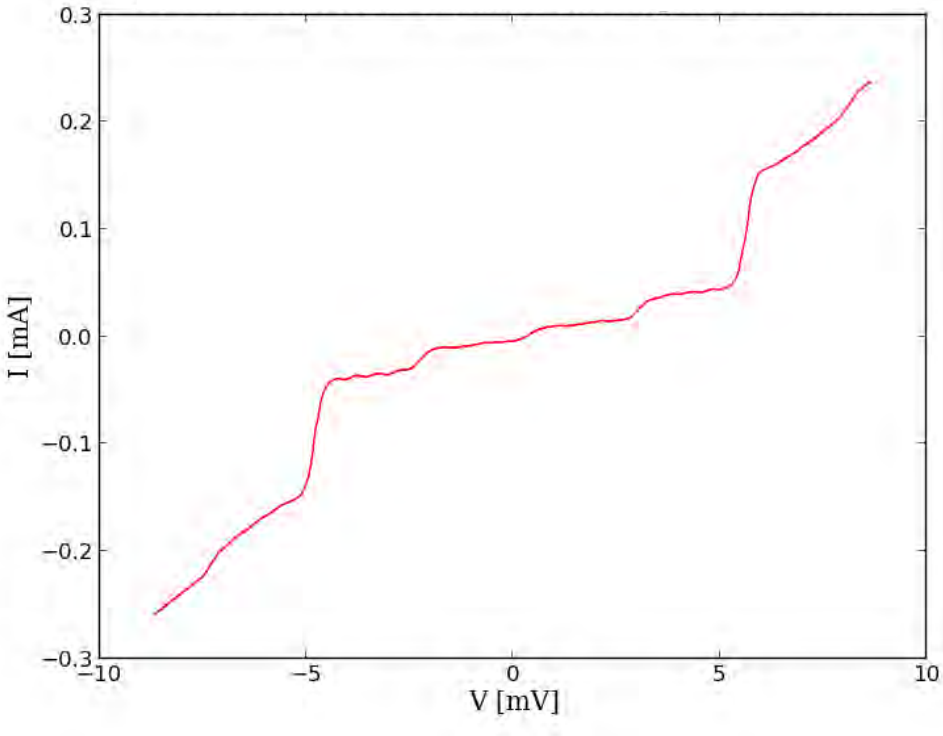

Figure 4.2.2: IV curve of the mixer lit by the local oscillator, and magnetic field effect.

3.4 Final IV Curve for the Mixer Fig. 4.2.2 shows the IV curve of the mixer lit by the local oscillator, but with a specific value of the magnetic field coils current that minimize the Josephson effects. Fig. 4.2.3 shows a comparison between the scan measurement and the data gathered from the oscilloscope.

4.3 Performance Analysis

4.3.1 Time Constant

After every instruction sent by the HAL layer (see section 3.2), the electronic board responds as an exponential decrease function in the time. This function has the form of Eq. 4.3.1, where K_1 and K_2 are constants, t the time and τ the time constant.

$$f(t) = K_1 \cdot e^{-\frac{t}{\tau}} + K_2 \tag{4.3.1}$$

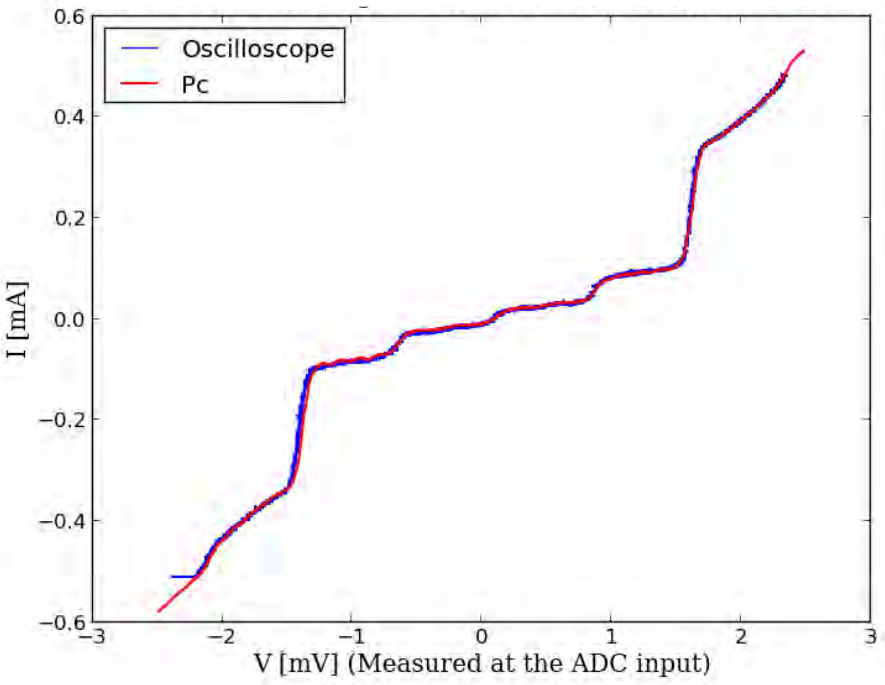

Figure 4.2.3: Oscilloscope-PC comparison of the IV curve of the mixer, lit by the local oscillator, and magnetic field effect.

Table 4.2: Values of electronic board time constant for three different installed capacitors.

Capacitor Value nF	Time Constant τ ms
320	0.57
570	1.1
1350	2.33

The time constant τ is an intrinsic property of an electronic system related to the construction method and the time response of all its components. However is possible to increase the value of this constant by placing a low pass filter in the electronic board. This procedure is done in order to diminish the electric noise since the filter behaves as an integrator in the time domain. With this purpose, a low pass filter with a capacitor of 570 nF was installed in the electronic board[2]. Table 4.2 shows the value of the time constant for this and another two values of the capacitor[3].

The values that were obtained for the time constant are the sum of the capacitor effect plus the intrinsic constant of the board. Assuming a linear dependence, is possible to model the final value of the time constant as the Eq. 4.3.2, where c is the value of the added capacitor, A the proportional constant and τ_0 the intrinsic value of the time constant for the electronic board. A linear fit over the values (see Appendix C.2) of the Table 4.2 returns: $A = 1.67727 \cdot 10^{-3}$ and $\tau_0 = 0.081$ ms.

[2]The decision to install the capacitor was made by the electronic group who designed the electronic board.
[3]These values were obtained using the dummy set-up (see Appendix C.1).

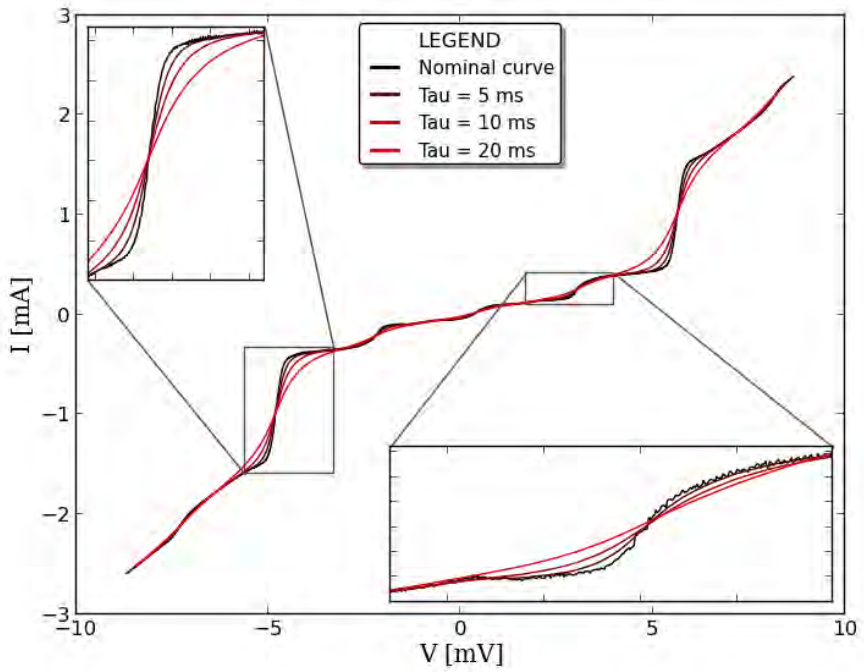

Figure 4.3.1: IV curve simulation for different values of the time constant.

$$\tau(c) = A \cdot c + \tau_0 \tag{4.3.2}$$

4.3.2 IV-Curve Distortion

Due to the decreasing exponential response of the electronic board, a delay appears in the shape of the measured curve when performing a sweep or a scan. This is because the instruction to go forward in any of the voltage steps occurs before the electronic board could reach the previously desired voltage value. To diminish this effect the average between the rise and decrease curve of the scan is taken. This led to the effects of the delay disappearing in some sectors and presenting a distortion of the shape in others. A simulation[4] of the distortion effects in the IV curve for different values of the time constant τ can be seen in Fig. 4.3.1. The simulation was made using the exponential response of Equation 4.3.1 over a nominal curve [5].

[4]The Appendix C.3 shows a comparison of the simulation with real measurements, using the dummy set-up, for different values of the time constant.

[5]This correspond to a distortion nominal curve and was obtained using the `BIAS_SCAN_SLOW` function (see Section 3.3.3). The delay introduced between every voltage step is long enough to allow the electronic board reach the desired value before the next instruction. Therefore the distortion effects are considerable low.

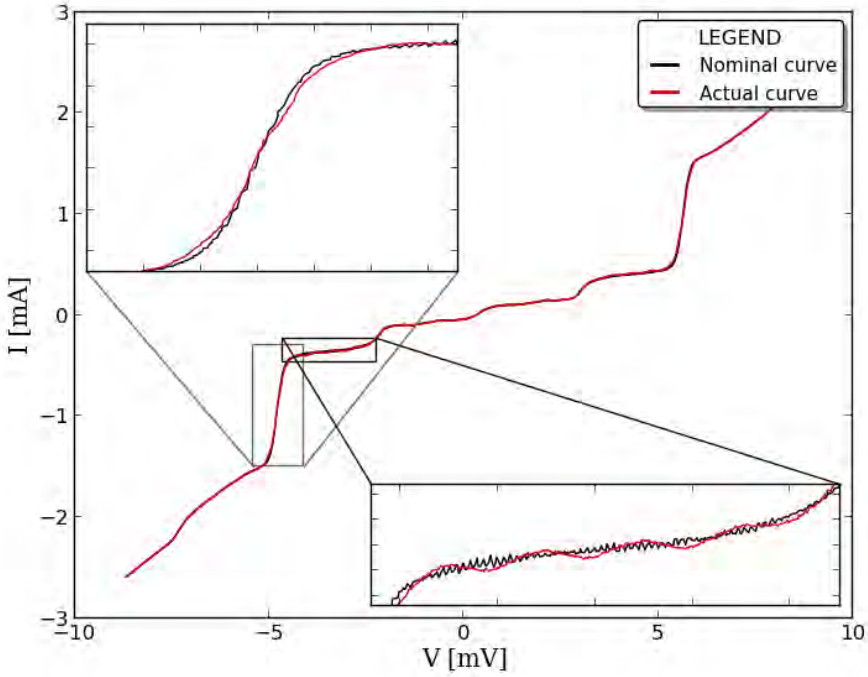

Figure 4.3.2: Comparison between nominal and actual IV curve for the mixer set-up.

4.3.3 Actual Distortion on the IV Curve

In the comparison between the actual and nominal IV curve, it is possible to distinguish the distortion mentioned above (left inset in Fig. 4.3.2). Even though this effect is present in every steep change of the current, the area where it is supposed to place the bias voltage (see Section 2.3) does not show signs of this type of distortion. However, it does have an oscillation (right inset in Fig. 4.3.2). A possible explanation is a transient effect after the steep changes of the current.

Chapter 5

Summary and Conclusion

In this thesis work we programmed the microprocessor of a prototype bias-control board to interact with an SIS mixer. The first part includes the system set-up, design, and programming of the software of the microprocessor. The second part is about the laboratory testing and performance analysis.

The system set-up and first iteration of the programming allowed us to improve the design of the electronic board in relation to the safe interaction with the mixer. The software was successfully programmed, and its functionality was tested in two different environments: dummy and mixer set-up. The dummy set-up was used to test the functions of the software, meanwhile the mixer set-up showed that a real IV curve can be obtained with this prototype bias-control board.

In terms of performance, the time constant of the board plays a fundamental role. It has direct influence on the processing time of the board, the electronic noise in the measurements, and the distortion of the IV curve. A smaller time constant will imply a faster response and less distortion in the IV curve, but will also increase the electronic noise in the measurements. The current time constant of the board was adequately measured. It was possible to identify the intrinsic and the low pass filter contribution. Nevertheless, the input from the mixer still needs to be measured in order to know the value of the entire system. This latter value will help to perform more accurate simulations of the curve shape distortion, and a nominal curve in terms of electronic noise. By comparing this nominal curve with the actual curve, it will be possible to measure the electronic noise.

The comparison between the actual and nominal curve (see Fig. 4.3.2) evinces that the distortion and electronic noise are within a very good range, due to the sector of the curve that is expected to tune the mixer (see Section. 2.3). Nevertheless, this generates a possibility in terms of efficiency, a trade off between the time response and the electronic noise.

In conclusion, the software programmed on the microprocessor creates a base of instructions that allows the bias-control board to safely interact with the mixer. This interaction permits the user to obtain and adjust the IV curve completely from the control PC; thereby allowing the user to perform a manual tuning of the mixer, obtaining the same results as the current process (see Section 2.3). This represents a step forward in replacing hardware complexity with software complexity, taking the bias-control electronics to a more integrated system; the latter is key for the development of large format heterodyne receivers.

5.1 Results Summary

5.1.1 Scaling Factor

Mixer I mA/count	Mixer V mV/count
$6.812615 \cdot 10^{-5}$	$5.308539 \cdot 10^{-4}$

Table 5.1.1: Scaling factor of the ADC for the current and voltage of the mixer

Using the ranges of voltage/current and counts given in Table 4.1, it was possible to measure the scaling factor of the physical quantity versus each count. The results are shown in Table 5.1.1.

5.1.2 Time Constant

Capacitor Value nF	Time Constant τ ms
320	0.57
570 (actual)	1.1
1350	2.33

Table 5.1.2: Values of electronic board time constant for three different installed capacitors

Table 5.1.2 shows the total value of the time constant (intrinsic plus low pass filter contribution) of the board for three different installed capacitors. By using a linear fit over the previous values it was possible to calculate the contribution of the board itself $\tau_0 = 0.081$ ms.

5.1.3 Final IV Curve of the Mixer

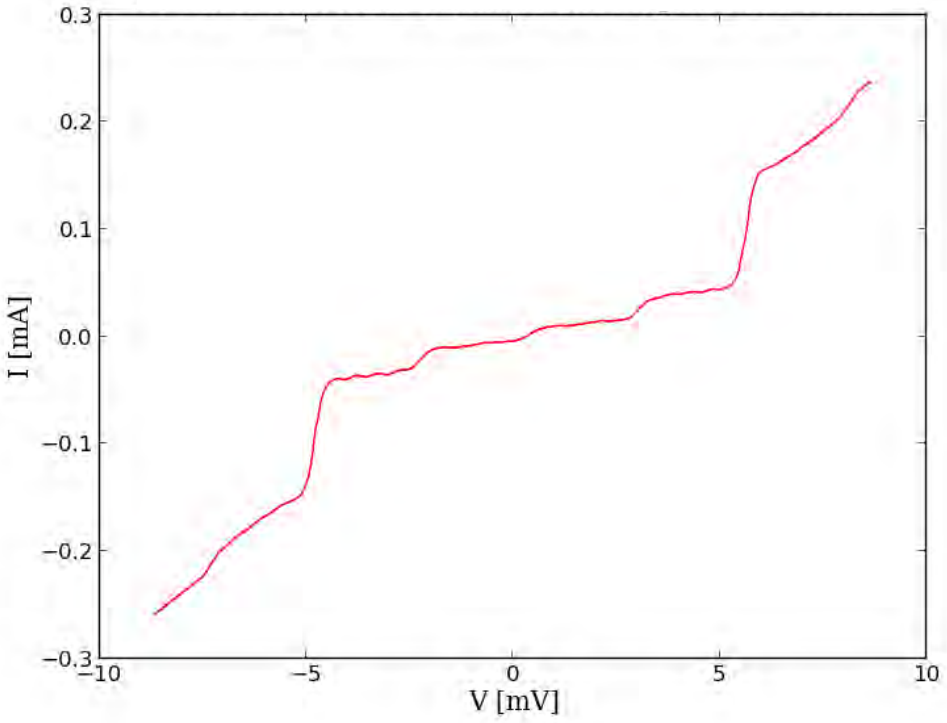

Figure 5.1.1: IV curve of the mixer lit by the local oscillator, and adjusted with magnetic field

Fig. 5.1.1 shows the final IV curve obtained from the real mixer, lit by the local oscillator and adjusted with the magnetic field to suppress the Josephson effects.

Bibliography

[1] History about ccat. CCAT Project. Last access in June-2015. [Online]. Available: http://www.ccatobservatory.org/index.cfm/page/about-ccat.htm

[2] (2013) Solar system studies with ccat. CCAT Project. Last access in June-2015. [Online]. Available: http://www.ccatobservatory.org/docs/ccat-posters-brochures/Lis%20&%20Bockelee_CCAT%20AAS%20Poster%20Jan2013.pdf

[3] J. R. Tucker, "Quantum limited detection in tunnel junction mixers," *IEEE Journal of Quantum Electronics*, vol. 15, pp. 1234–1258, Nov. 1979.

[4] V. Vassilev, "Development of a sideband separating sis mixer technology for mm-wavelengths," Ph.D. dissertation, Chalmers University of Technology, 2003.

[5] J. Bardeen, L. N. Cooper, and J. R. Schrieffer, "Theory of Superconductivity," *Physical Review*, vol. 108, pp. 1175–1204, Dec. 1957.

[6] J. Kooi, "Advanced receivers for submillimeter and far infrared astronomy," Ph.D. dissertation, University of Groningen, 2008.

[7] B. D. Josephson, "Possible new effects in superconductive tunnelling," *Physics Letters*, vol. 1, pp. 251–253, Jul. 1962.

[8] S. Shapiro, "Josephson Currents in Superconducting Tunneling: The Effect of Microwaves and Other Observations," *Physical Review Letters*, vol. 11, pp. 80–82, Jul. 1963.

[9] S. Stanko, U. U. Graf, and S. Heyminck, "Automatic Tuning of SMART, KOSMA's 490/810 GHz Array Receiver," in *Thirteenth International Symposium on Space Terahertz Technology*, Mar. 2002, pp. 421–430.

[10] C. Walker, C. Groppi, D. Golish, C. Kulesa, A. Hungerford, and C. Drouet d'Aubigny, "PoleStar: An 810 GHz Array Receiver for AST/RO," in *Twelve International Symposium on Space Terahertz Technology*, 2001.

[11] U. U. Graf, S. Heyminck, E. A. Michael, S. Stanko, C. E. Honingh, K. Jacobs, R. T. Schieder, J. Stutzki, and B. Vowinkel, "SMART: The KOSMA Sub-Millimeter Array Receiver for Two frequencies," in *Millimeter and Submillimeter Detectors for Astronomy*, ser. Society of Photo-Optical Instrumentation Engineers (SPIE) Conference Series, T. G. Phillips and J. Zmuidzinas, Eds., vol. 4855, Feb. 2003, pp. 322–329.

[12] C. Groppi, C. Walker, C. Kulesa, D. Golish, D. Hedden, P. Gensheimer, G. Narayanan, A. Lichtenberger, U. Graf, and S. Heyminck, "Desert STAR: a 7 pixel 345 GHz Heterodyne Array Receiver for the Heinrich Hertz Telescope ," 2003.

[13] K.-F. Schuster, C. Boucher, W. Brunswig *et al.*, "A 230 GHz heterodyne receiver array for the IRAM 30 m telescope," 2004.

[14] C. E. Groppi, C. Walker, C. Kulesa, D. Golish, J. Kloosterman, S. Weinreb, G. Jones, J. Barden, H. Mani, J. Kooi, T. Kuiper, A. Lichtenberger, T. Cecil, A. Hedden, G. Narayanan, and P. Puetz, "Supercam: A 64-Pixel Array Receiver for the 870 micron Atmospheric Window," in *American Astronomical Society Meeting Abstracts #215*, 2010.

Appendix A

Microprocessor Programming

A.1 Hexadecimal Command List

```
/*! \file commands.h

    List of commands to communicate with bias electronics frontend

    Command structure:
    <address><code><parameters>

    <address>:
binary list of desired channels, e.g. 0x0C for channels 2,3
    <code>:       command byte (see below)
    <parameter>: required parameter(s) if any

    \author Pablo Tapia U (tapia@ph1.uni-koeln.de)

    \date started in 2014
*/


/* Bias Settings */
#define SET_BIAS_VOLTAGE    0x10
#define GET_BIAS_SETTINGS   0x11

/* Magnet Current */
```

```
#define SET_MAGNET_CURRENT 0x20
#define GET_MAGNET_CURRENT 0x21

/* LNA bias */
#define SET_LNA_VOLTAGE_A  0x30
#define GET_LNA_VOLTAGE_A  0x31
#define SET_LNA_VOLTAGE_B  0x32
#define GET_LNA_VOLTAGE_B  0x33

/* Mixer status */
#define MIXER_STATUS       0x40
#define ENABLE_MIXER       0x41
#define DISABLE_MIXER      0x42

/* Sweeps */
#define STOP_SWEEP         0x50
#define START_BIAS_SWEEP   0x51
#define START_MAGNET_SWEEP 0x52
#define BIAS_SCAN          0x53
#define MAGNET_SCAN        0x54
#define BIAS_SCAN_SLOW     0X55

/*Miscellaneous*/
#define TEST               0xFA
#define TOGGLE_DEBUG       0xFD
#define STATUS             0xFE
#define RESET              0xFF
#define SET_CHANNEL        0xF0
#define GET_CHANNEL        0XF1
#define RELAY_ENABLE       0XF2
#define RELAY_DISABLE      0XF3
```

Appendix B

Laboratory Testing

B.1 Dummy Set-Up Value Response

Table B.1.1: Analog and digital values of the mixer voltage and current, corresponding to different values of the DAC determined by the Control PC.

DAC		Mixer I	ADC		Mixer V	ADC	
Value	Output[V]	I [mA]	Input[V]	Value	V[mV]	Input[V]	Value
0	-2.503	+0.89	-2.011	-13203	-8.7	-2.492	-16366
1000	-1.285	+0.46	-1.037	-6824	-4.5	-1.279	-8420
2047	-0.009	+0.0	-0.019	-134	-0.1	-0.019	-720
2054	+0.0	+0.0	-0.012	-98	+0.0	+0.0	-140
2500	+0.543	-0.19	+0.422	+2750	+1.9	+0.541	+3534
4095	+2.487	-0.89	+1.975	+12925	+8.6	+2.476	+16223

B.2 IV Curves for the Mixer Set-Up

B.2.1 Initial IV Curve

B.2.2 IV Curve with Magnetic Field Effect

B.2.3 Effect of the Local Oscillator on the IV Curve

B.2.4 Oscilloscope Screenshot for the Final IV Curve

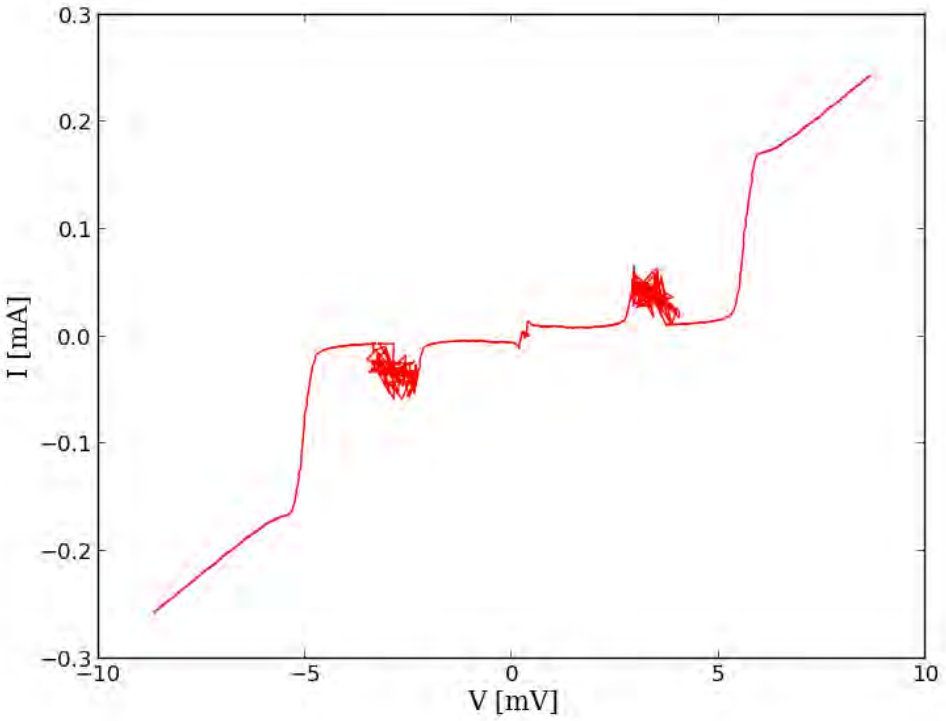

Figure B.2.1: Initial IV curve of the mixer.

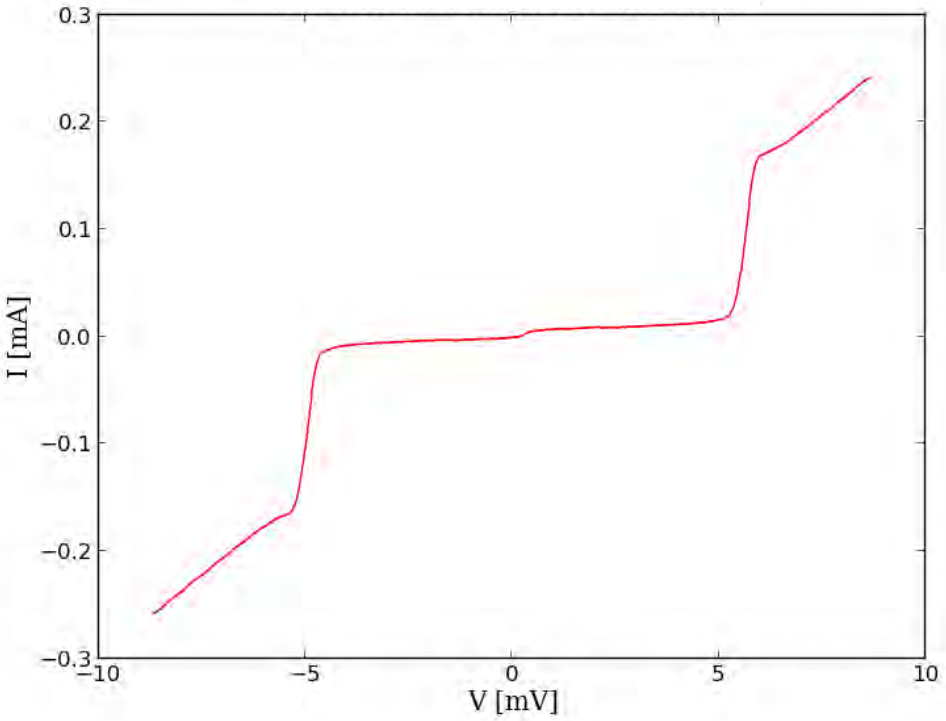

Figure B.2.2: IV curve of the mixer with magnetic field effect .

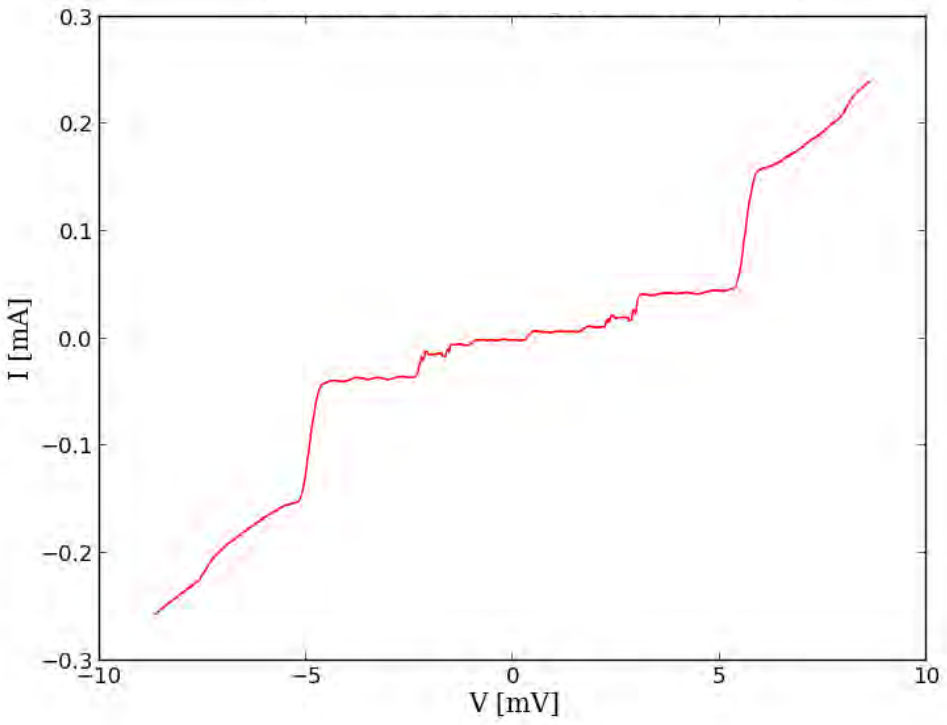

Figure B.2.3: IV curve of the mixer lit by the local oscillator.

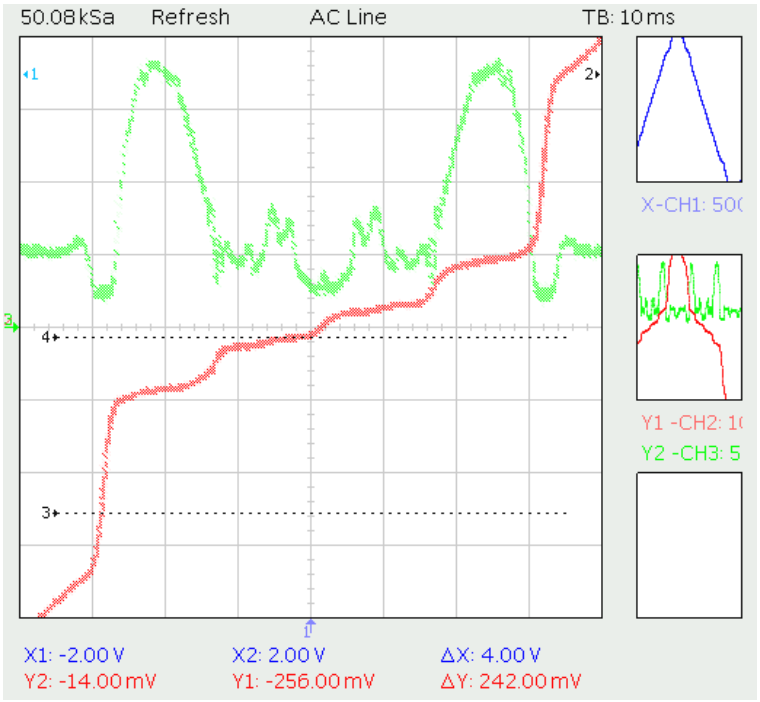

Figure B.2.4: Oscilloscope screenshot of the IV curve of the mixer, lit by the local oscillator, and magnetic field effect.

Appendix C

Performance Analysis

C.1 Method to Obtain the Time Constant

Using the dummy set-up, an experiment was performed in order to determined the time constant of the electronic board. The mixer bias-voltage was placed in the maximum value and take it to the lowest possible in a single instruction. Fig. C.1.1 shows the fit function over the response of the voltage (measured at the ADC input). This fit was calculated using a programmed function for the Equation 4.3.1.

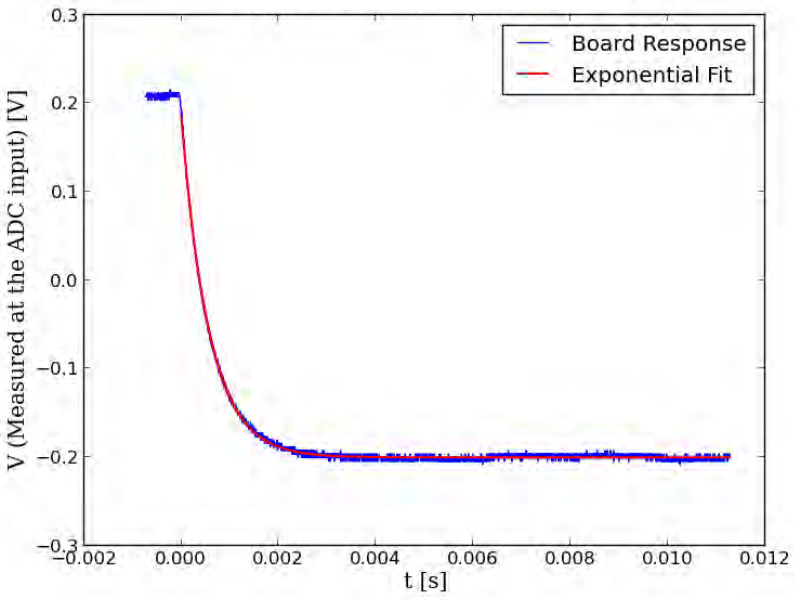

Figure C.1.1: Exponential fit over the response of the wider voltage step in the electronic board.

C.2 Linear Fit Over Experimental Values of the Time Constant

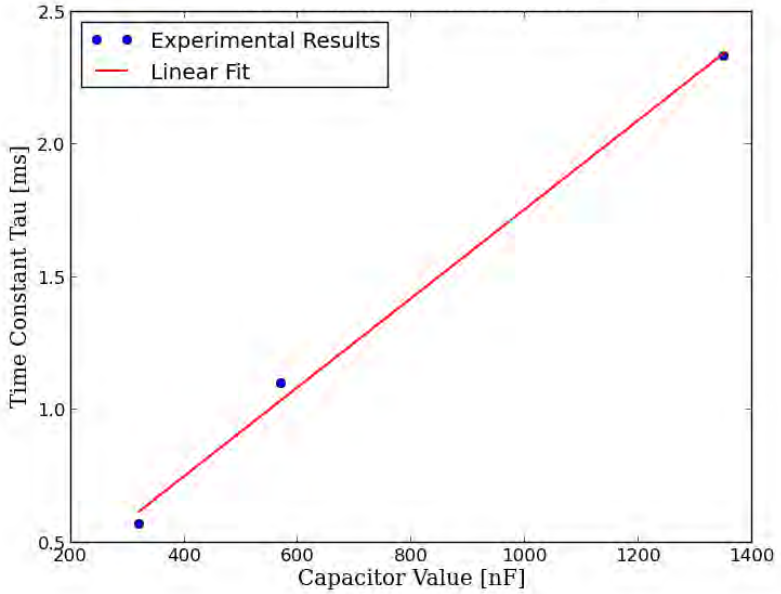

Figure C.2.1: Linear fit over the experimental values for the time constant τ. Experiment made with three different capacitors for the low pass filter of the electronic board.

C.3 Curve Shape Distortion Simulation

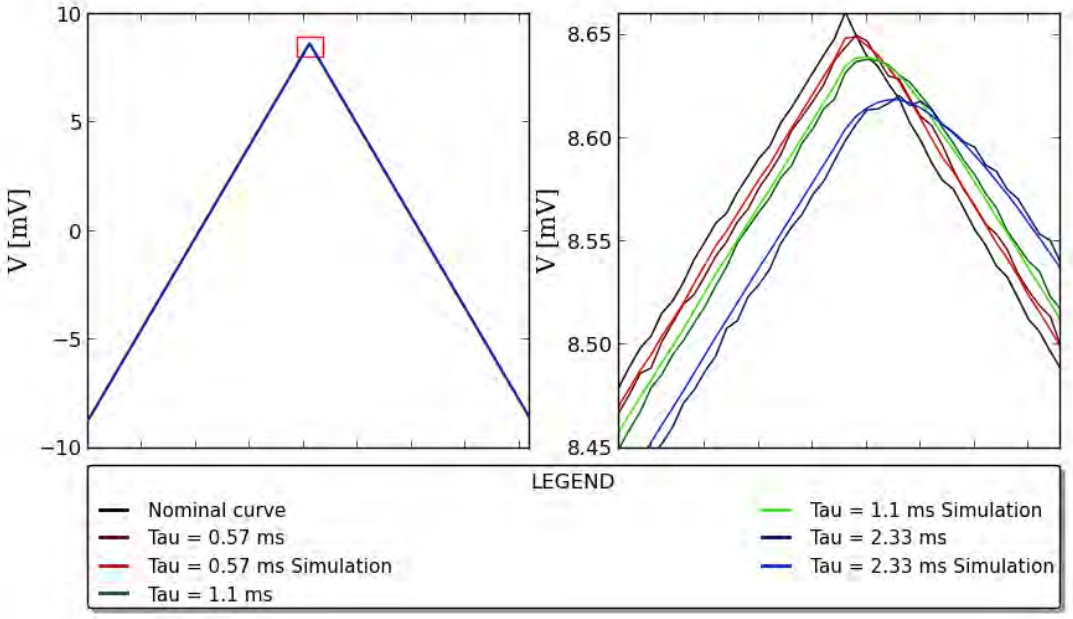

Figure C.3.1: Comparison between real and simlutated IV curves, for different time constants Tau.